1-1-2010

Structural analysis of proteins by isotope-edited FTIR spectroscopy

Suren A. Tatulian
University of Central Florida

Spectroscopy 24 (2010) 37–43
DOI 10.3233/SPE-2010-0412
IOS Press

Structural analysis of proteins by isotope-edited FTIR spectroscopy

Suren A. Tatulian *
Department of Physics, University of Central Florida, Orlando, FL, USA

Abstract. Structure determination of multidomain proteins or protein–membrane complexes is one of the most challenging tasks in modern structural biology. High-resolution techniques, like NMR or X-ray crystallography, are limited to molecules of moderate size or those that can be crystallized easily. Both methods encounter serious technical obstacles in structural analysis of protein–membrane systems. This work describes an emerging biophysical technique that combines segmental isotope labeling of proteins with Fourier transform infrared (FTIR) spectroscopy, which provides site-specific structural information on proteins and allows structural characterization of protein–membrane complexes. Labeling of a segment of the protein with ^{13}C results in infrared spectral resolution of the labeled and unlabeled parts and thus allows identification of structural changes in specific domains/segments of the protein that accompany functional transitions. Segmental isotope labeling also allows determination of the precise configuration of protein–membrane complexes by polarized attenuated total reflection FTIR (ATR–FTIR) spectroscopy. These new developments offer solutions to functionally important site-specific structural changes in proteins and protein–membrane complexes that are hard to approach using conventional methods.

Keywords: Protein engineering, protein structure, infrared spectroscopy, isotope labeling, phospholipase A_2

1. Introduction

Proteins often carry out their specific functions by forming complexes with other proteins, nucleic acids, membranes or other cell components. Determination of the structures of these complexes is key to understanding the molecular mechanisms underlying protein function. While the most valuable structural information on macromolecular complexes has been provided by atomic-resolution techniques such as X-ray crystallography and NMR, structural characterization of protein–membrane complexes is a particularly challenging problem for both methods [3,6,8,10,11,15]. Therefore, there is an urgent need to develop new biophysical or other technologies to characterize the structure and dynamics of proteins in their membrane-bound state and to resolve structural changes occurring in specific domains or segments of the protein.

Infrared spectroscopy is an inherently versatile biophysical tool for structural analysis of protein complexes [1,2,17]. This method is not limited to the molecular size and can provide structural information on all components of the system, e.g., proteins, lipids, nucleic acids, etc., without the need of labeling the molecules with spectroscopic probes. However, conventional FTIR spectroscopy is unable to distinguish between structural changes taking place in individual proteins in a complex or different domains of a protein during functional transitions. Although polarized ATR–FTIR spectroscopy allows determination of the orientation of simple molecules, such as lipids, peptides, and proteins that have a rotational

* Address for correspondence: Suren A. Tatulian, Department of Physics, University of Central Florida, 4000 Central Florida Blvd., Orlando, FL 32816, USA. Tel.: +1 407 823 6941; Fax: +1 407 823 5112; E-mail: tatulian@physics.ucf.edu.

symmetry axis, meaningful orientational information cannot be obtained for membrane-bound proteins of complex, irregular structures [17].

The purpose of this work was to demonstrate that the combination of segmental isotope labeling of proteins with FTIR spectroscopy can solve the above mentioned drawbacks and provide both site-specific structural information and the precise mode of protein–membrane interactions. This method has been applied to a membrane-binding protein, human pancreatic phospholipase A_2 (PLA_2). PLA_2 enzymes undergo a substantial increase in their phospholipid hydrolyzing activity upon binding to cellular membranes [4,9], yet the structural aspects of the interfacial activation remain uncharacterized. The N-terminal α-helix of certain secreted PLA_2s, including pancreatic PLA_2, has been shown to play an important regulatory role in the enzyme function [12,13,19]. Here, peptide ligation was used to produce a semisynthetic human pancreatic PLA_2 in which the N-terminal helix was unlabeled while the rest of the protein was ^{13}C-labeled. The segmentally isotope labeled PLA_2 was studied by direct transmission and ATR–FTIR spectroscopy to identify the structural dynamics of the labeled and unlabeled parts of the protein as well as to determine the precise membrane binding mode of PLA_2.

2. Materials and methods

All lipids were purchased from Avanti Polar Lipids, Inc. (Alabaster, AL, USA) and most of the other chemicals were from Sigma-Aldrich (St. Louis, MO, USA). The N-terminal decapeptide of human pancreatic PLA_2 containing a C-terminal thioester group (Ala-Val-Trp-Gln-Phe-Arg-Lys-Met-Ile-Lys-$COSCH_2COOH$) was synthesized by SynPep Corp. (Dublin, CA, USA). The fragment of PLA_2 Cys^{11}–Ser^{126}, named ΔN10, was expressed in *Escherichia coli* in an M9 minimal medium containing 0.2% $^{13}C_6$-D-glucose as a sole metabolic source of carbon so as to produce a uniformly ^{13}C-labeled recombinant protein.

The segmentally ^{13}C-labeled PLA_2 was engineered by using the thioester-to-cysteine peptide ligation strategy [5,16]. The thioesterified peptide was incubated with the ^{13}C-labeled fragment ΔN10 in the denaturing buffer (6 M guanidinum-HCl, 100 mM Na-phosphate, 5% β-mercaptoethanol, 1 mM EDTA, pH 7.4) supplemented with 4 vol% thiophenol and 4 vol% benzyl mercaptan. The reaction was allowed to proceed for 6 h at 20°C. Under properly selected reducing conditions (see above), the C-terminal thioester group of the unlabeled peptide reacts with the side-chain thiol group of the N-terminal cysteine of the ^{13}C-labeled ΔN10 fragment of PLA_2, which is followed by a rapid and irreversible S-to-N acyl shift to regenerate the thiol group of Cys^{11} and simultaneously form a native peptide bond at the ligation site. The ligated sample was diluted 10-fold in the denaturing buffer, and 5 mM Tris (2-carboxyethyl) phosphine hydrochloride was added to reduce disulfides between internal cysteines of PLA_2 and thiophenol and/or benzyl mercaptan [16]. The protein was refolded by dialysis and purified using ion exchange and size exclusion column chromatography, as described [12,13,19]. The semisynthetic PLA_2 was identified by immunoblotting and had nearly the same specific phospholipid hydrolyzing activity as the recombinant PLA_2.

The segmentally ^{13}C-labeled PLA_2 was structurally characterized by FTIR spectroscopy, using a Vector 22 infrared spectrometer (Bruker Optics, Billerica, MA, USA), equipped with an aluminum grid polarizer (Specac, Suffolk, UK) and ATR accessories (Buck Scientific, East Norwalk, CT, USA). For direct transmission measurements of the free protein in the absence of lipid, the lyophilized PLA_2 sample was dissolved in a D_2O-based buffer (100 mM NaCl, 1 mM NaN_3, 1 mM EGTA, 50 mM Hepes, pD 7.4), 70 μl of the protein solution was placed between two CaF_2 windows, using a 25 μm Teflon spacer, and consecutive spectra were measured during 2 h (200 scans per spectrum), as described [12].

Supported phospholipid bilayers were prepared on a germanium internal reflection plate (Harrick Scientific, Pleasantville, NY, USA), using a Langmuir–Blodgett trough (model 611, Nima Technology, Coventry, UK), as described in more detail earlier [12,13]. The bilayer composition was 80 mol% 1-palmitoyl-2-oleoyl-*sn*-glycero-3-phosphocholine (POPC) and 20 mol% 1-palmitoyl-2-oleoyl-*sn*-glycero-3-phosphoglycerol (POPG). For polarized ATR–FTIR measurements on the membrane-bound PLA_2, the protein solution in the same D_2O-based buffer (see above) was injected into the ATR cell containing a pre-formed supported phospholipid membrane and consecutive spectra were measured during 2 h using infrared radiation at parallel or perpendicular polarizations relative to the incidence plane. All spectra were recorded at a 2 cm^{-1} nominal resolution, at 20°C. For secondary structure determination, the polarized spectra were used to obtain "polarization-independent" spectra: $A = A_{\parallel} + 0.8A_{\perp}$ (see [17] for details). The fraction of each secondary structure element, e.g. α-helix, was evaluated as the fraction of the respective amide I component relative to the total amide I area [12]. The kinetics of amide hydrogen/deuterium exchange (HX) was quantitatively characterized based on spectral changes in the amide I region, as described [18]. The time dependence of HX was described using a double-exponential formalism, which presents the fraction of unexchanged residues at time t as follows:

$$\frac{[H]}{[H]+[D]} = a_0 + a_1 e^{-k_1 t} + a_2 e^{-k_2 t}, \tag{1}$$

where $[H]$ and $[D]$ are the fractions of the amide groups in the H and D forms at time t, respectively, a_0, a_1 and a_2 are the fractions of HX-resistant, slow exchanging and fast exchanging amino acid residues, respectively, and k_1 and k_2 are the rate constants of slow- and fast-exchanging residues.

3. Results and discussion

Since the N-terminal α-helix of pancreatic PLA_2 is believed to play a regulatory role in activation of the enzyme upon membrane binding [12–14], it was important to elucidate the structural dynamics of the N-terminal helix and the rest of the protein during membrane binding. In order to resolve the conformational changes occurring in different regions of PLA_2, a semisynthetic PLA_2 was created in which the N-terminal helix was not labeled (shown in magenta in Fig. 1(A)) whereas the rest of the protein was ^{13}C-labeled (see Section 2). The purified, segmentally ^{13}C-labeled PLA_2 was studied by FTIR spectroscopy, both free in the buffer in the absence of lipid (not shown) and bound to supported bilayers (Figs 1 and 2). Figure 1(B) and (C) show the ATR–FTIR spectra of the membrane-bound PLA_2 in the amide I region and their 2nd derivatives at different times of exposure to D_2O. Initially, at 15 min of exposure to D_2O, the 2nd derivative of the amide I spectrum shows two components at 1657 and 1618 cm^{-1} (dark blue line in Fig. 1(C)), which are assigned to the unlabeled N-terminal α-helix and the ^{13}C-labeled internal helices, respectively. These components undergo gradual downshift by 7–8 cm^{-1} upon HX for 2 h. A $\sim$40 cm^{-1} shift of the amide I signal toward lower wavenumbers resulting from ^{13}C-labeling is consistent with results obtained on synthetic peptides [21] and provides a unique opportunity for conformational characterization of defined segments of the protein.

The amide I band of a segmentally isotope labeled protein in a D_2O-based buffer is a combination of components generated by various secondary structure types of both unlabeled and labeled segments, all of which undergo spectral shifts due to amide HX at different rates. This results in a dynamically transforming complex picture, as shown in Fig. 1(B) and (C). The total number of α-helical residues

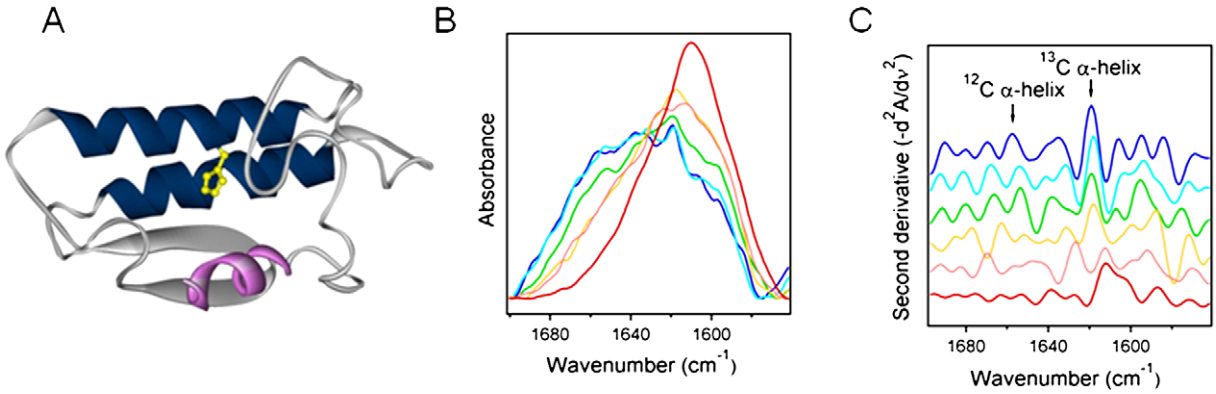

Fig. 1. (A) The ribbon presentation of the structure of human pancreatic PLA_2. The N-terminal helix is shown in magenta, the two internal helices in dark blue, and the catalytic His^{48} in yellow, in a ball and stick format. (B) ATR–FTIR spectra of semisynthetic PLA_2 in which the N-terminal α-helix is unlabeled and the rest of the protein is ^{13}C-labeled, reconstituted in supported POPC/POPG (4:1) bilayer membranes. The spectra were obtained using those measured at parallel and perpendicular polarizations of the infrared light as $A = A_{\parallel} + 0.8A_{\perp}$. Change of color from blue to red corresponds to increasing time of exposure of the protein to D_2O (15, 30, 40, 60, 120 min and 19 h). (C) The inverted second derivatives of spectra in the amide I region (the color code is the same as in panel B). (The colors are visible in the online version of the article.)

in PLA_2 is 41, implying that the expected ratio of the amide I areas of the unlabeled N-terminal α-helix (10 residues) and the ^{13}C-labeled helical residues (31 residues) would be 0.32, assuming equal extinction coefficients for the unlabeled and ^{13}C-labeled residues. However, the area of the component at 1657–1650 cm^{-1}, corresponding to the unlabeled N-terminal α-helix, is considerably larger than expected, indicating a decrease in the extinction coefficient upon ^{13}C-labeling. The results of curve-fitting of amide I spectra at different times of HX (Fig. 2) allowed evaluation of the ratio of extinction coefficients of ^{13}C-labeled and unlabeled helices, $\varepsilon_{13C}/\varepsilon_{12C} = 0.62 \pm 0.27$. This result accords, within the range of experimental error, with $\varepsilon_{13C}/\varepsilon_{12C} = 0.7$–$0.8$ determined for synthetic peptides with segmentally ^{13}C-labeled backbone carbonyls [21].

The positions of all amide I components were identified by 2nd derivative spectra (Fig. 1(C)) and were used for deconvolution of the amide I bands (Fig. 2). Data of Figs 1(C) and 2 demonstrate the dynamics of the deuteration of the amide protons of PLA_2. Initially, the amide I band is a wide and complex envelope and with progression of HX it undergoes narrowing and spectral downshift. Each amino acid residue of the protein can undergo amide HX with its individual rate constant, determined by local mobility, H-bonding and steric protection from the solvent [7]. However, the residues involved in a given secondary structure, e.g. an α-helix, usually have similar HX rates [18], which allows one to monitor the individual rates of HX of the N-terminal and the internal α-helices of PLA_2. In case of uneven deuteration rates at different parts of a helix, the helical amide I component can be split. This effect was detected for the N-terminal helix of PLA_2 at 60 min of HX (Fig. 2(E)).

Comparison of the amide I spectra of the segmentally ^{13}C-labeled PLA_2 free in buffer and bound to supported phospholipid bilayers allowed identification of site-specific changes in the secondary structure and the dynamics of the protein upon membrane binding. Comparison of the total α-helical content of the free PLA_2 with that of the membrane-bound protein indicates a 5% (6 residues) reduction in the α-helical content. This effect is consistent with structural changes occurring in porcine pancreatic PLA_2

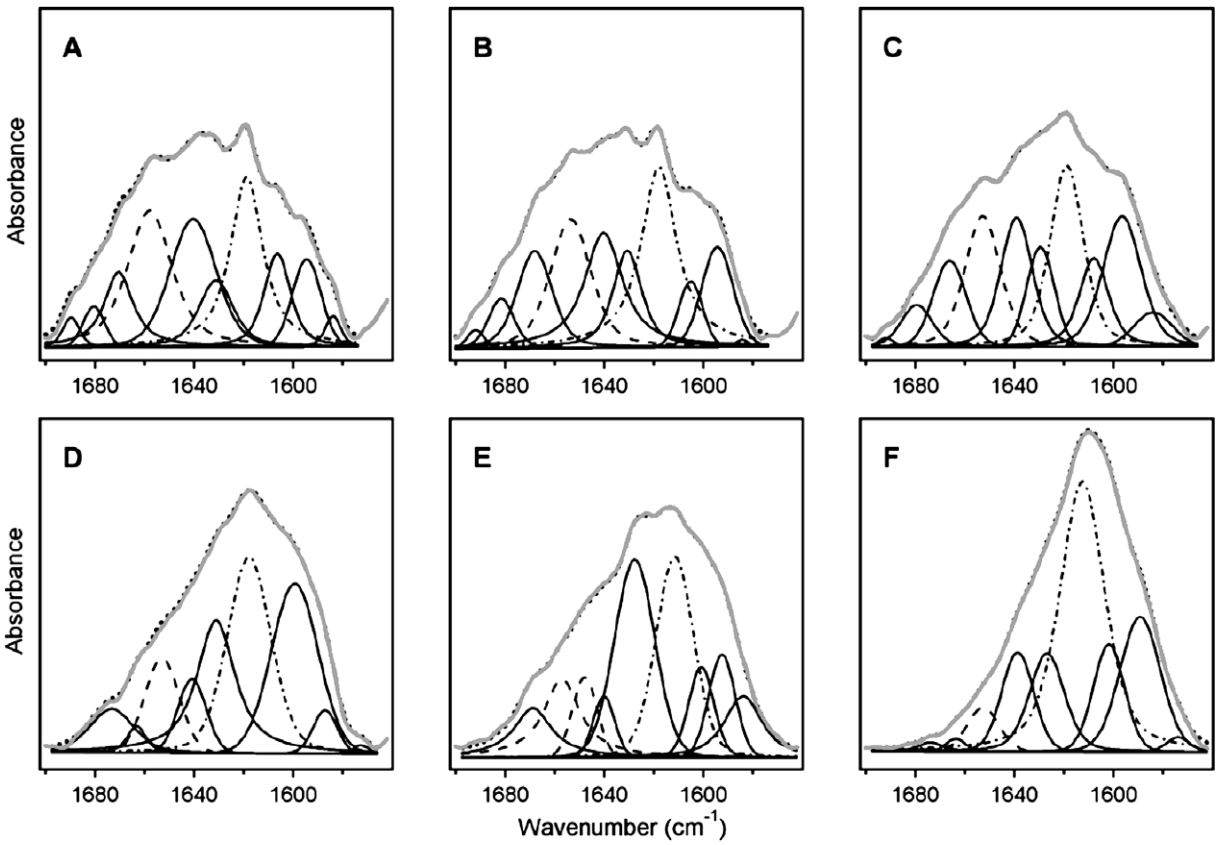

Fig. 2. ATR–FTIR absorbance spectra of human pancreatic PLA_2 reconstituted in supported POPC/POPG (4:1) bilayers. The sample has been exposed to a D_2O-based buffer for 15, 30, 40, 60, 120 min and 19 h (panels A–F, respectively). The grey lines are the experimentally measured spectra. The components under the amide I envelope have been obtained by curve-fitting, using the component wavenumbers identified by the 2nd derivatives (Fig. 1(C)). The dotted line is the sum of all components; its coincidence with the experimental spectrum (grey line) indicates the goodness of the curve-fitting. The dashed component has been assigned to the unlabeled N-terminal helix, and the dashed-dotted line to the internal, ^{13}C-labeled helices.

upon binding to phospholipid micelles identified by NMR [20] and can be interpreted in terms of an overall increased motional flexibility of interfacially activated PLA_2.

The amide HX kinetics of the N-terminal helix and the internal helices of free and membrane-bound PLA_2 were determined based on time-dependent spectral shifts of corresponding amide I components, using Eq. (1). The results, summarized in Table 1, indicate that the fractions of the HX-resistant and slow-exchanging residues in the N-terminal helix increase, the fraction of fast exchanging residues decreases, and both rate constants decrease upon membrane binding. In contrast, during membrane binding the fractions of dynamically distinct populations of amino acid residues in the internal helices undergo slight changes, but both HX rate constants increase. These data allow differentiation of the dynamic structural changes in the N-terminal and the internal helices of PLA_2 during the process of membrane binding, which under catalytic conditions (presence of Ca^{2+}) lead to the enzyme activation. The results are consistent with stabilization of the N-terminal helix of the protein and transition of the internal helices to a more flexible conformational state upon membrane binding. Interestingly, NMR studies on

Table 1

The parameters of amide hydrogen exchange of the N-terminal helix and the internal helices of human pancreatic PLA_2 free in the buffer and bound to POPC/POPG (4:1) membranes. In both cases, the buffer was 100 mM NaCl, 1 mM NaN_3, 1 mM EGTA, 50 mM Hepes in D_2O, pD 7.4

	Free in buffer		Membrane-bound	
	N-terminal	Internal	N-terminal	Internal
a_0	0.13	0.08	0.21	0.06
a_1	0.39	0.36	0.44	0.41
a_2	0.48	0.56	0.35	0.53
k_1 (min^{-1})	0.16	0.07	0.04	0.20
k_2 (min^{-1})	2.08	2.56	1.35	4.75

a porcine pancreatic PLA_2, which shares 88% sequence identity with its human counterpart, identified that the N-terminal helix of PLA_2 acquires a rigid structure in the complex with phospholipid micelles and a substrate mimic [20], which is consistent with our findings.

In addition to characterization of the dynamic structural properties of the protein, polarized ATR–FTIR spectra of the segmentally ^{13}C-labeled PLA_2 were used to determine the precise membrane binding mode of the protein, which has been described elsewhere [19].

4. Conclusions

Combination of segmental isotope labeling of proteins with FTIR spectroscopy is a novel biophysical approach that provides site-specific structural and dynamic information on proteins and their complexes. Labeling of a whole segment of the protein generates more reliable results compared to labeling of one or a few amino acids because in the latter case the relatively weak signal and transition dipole coupling between ^{12}C- and ^{13}C-amino acids obscures the signal from the labeled residues and thereby impairs the conformational information contained in it. Besides the site-specific structural information, this approach allows determination of the angular orientation of membrane-bound proteins and thus provides insight into the molecular details of membrane protein function.

References

[1] I.T. Arkin, *Curr. Opin. Chem. Biol.* **10** (2006), 394–401.
[2] A. Barth, *Biochim. Biophys. Acta* **1767** (2007), 1073–1101.
[3] F. Basyn, B. Spies, O. Bouffioux, A. Thomas and R. Brasseur, *J. Mol. Graph. Model.* **22** (2003), 1–21.
[4] O.G. Berg, M.H. Gelb, M.-D. Tsai and M.K. Jain, *Chem. Rev.* **101** (2001), 2613–2653.
[5] U.K. Blaschke, J. Silberstein and T.W. Muir, *Methods Enzymol.* **328** (2000), 478–496.
[6] M. Caffrey and V. Cherezov, *Nat. Protoc.* **4** (2009), 706–731.
[7] S.W. Englander, *Annu. Rev. Biophys. Biomol. Struct.* **29** (2000), 213–238.
[8] C. Hunte and S. Richers, *Curr. Opin. Struct. Biol.* **18** (2008), 406–411.
[9] G. Lambeau and M.H. Gelb, *Annu. Rev. Biochem.* **77** (2008), 495–520.
[10] A.G. Lee, *Biochim. Biophys. Acta* **1612** (2003), 1–40.
[11] D. Mustafi and K. Palczewski, *Mol. Pharmacol.* **75** (2009), 1–12.
[12] S. Qin, A.H. Pande, K.N. Nemec and S.A. Tatulian, *J. Mol. Biol.* **344** (2004), 71–89.
[13] S. Qin, A.H. Pande, K.N. Nemec, X. He and S.A. Tatulian, *J. Biol. Chem.* **280** (2005), 36773–36783.
[14] S. Ray, J.L. Scott and S.A. Tatulian, *Biochemistry* **46** (2007), 13089–13100.
[15] C.R. Sanders and F. Sönnichsen, *Magn. Reson. Chem.* **44** (2006), S24–S40.
[16] J.P. Tam, Q. Yu and Y.A. Lu, *Biologicals* **29** (2001), 189–196.

[17] S.A. Tatulian, *Biochemistry* **42** (2003), 11898–11907.
[18] S.A. Tatulian, D. Cortes and E. Perozo, *FEBS Letters* **423** (1998), 205–212.
[19] S.A. Tatulian, S. Qin, A.H. Pande and X. He, *J. Mol. Biol.* **351** (2005), 939–947.
[20] B. van den Berg, M. Tessari, R. Boelens, R. Dijkman, G.H. de Haas, R. Kaptein and H.M. Verheij, *Nat. Struct. Biol.* **2** (1995), 402–406.
[21] S.Y. Venyaminov, J.F. Hedstrom and F.G. Prendergast, *Proteins* **45** (2001), 81–89.